# Sensitivity of the Channel $pp \to ppWWH$ to Beyond Standard Model Couplings

Avi Shah

January 26, 2025

**Abstract**

The discovery of the Higgs boson at CERN's Large Hadron Collider (LHC) confirmed the mechanism by which particles acquire mass, the last fundamental particle foreseen by the Standard Model. Despite its success, the Standard Model leaves many fundamental questions unanswered, including the origin of the universe's matter-antimatter asymmetry. One possibility to address these gaps lies in exploring deviations in the properties of the Higgs boson with respect to the Standard Model predictions, particularly its couplings to other particles. This study focuses on anomalous interactions between the Higgs boson and W bosons (HWW couplings), which could provide evidence of new physics beyond the Standard Model. By modifying the charge-parity (CP) properties of the Higgs boson within the SMEFTsim framework and simulating these interactions using MadGraph, we aim to identify possible observables sensitive to the Higgs CP quantum number that can be used in the future with ATLAS data to probe such anomalous interactions.

# Contents

# 1 Introduction

## 1.1 The Standard Model

The Standard Model, or SM, of Particle Physics codifies and relates elementary particles and forces of our universe. Although it leaves some questions unanswered [1], this framework has proven to be an extremely useful theory for the modelling and subsequent prediction of interactions in the subatomic world between the set of fundamental, indivisible particles presented in Table 1.

| **Category** | **Particle** | **Symbol** | **Properties** |
|---|---|---|---|
| **Quarks** | Up | $u$ | Charge: $+\frac{2}{3}$, Mass: $\sim 2.2$ MeV |
| | Down | $d$ | Charge: $-\frac{1}{3}$, Mass: $\sim 4.7$ MeV |
| | Charm | $c$ | Charge: $+\frac{2}{3}$, Mass: $\sim 1.28$ GeV |
| | Strange | $s$ | Charge: $-\frac{1}{3}$, Mass: $\sim 96$ MeV |
| | Top | $t$ | Charge: $+\frac{2}{3}$, Mass: $\sim 173$ GeV |
| | Bottom | $b$ | Charge: $-\frac{1}{3}$, Mass: $\sim 4.18$ GeV |
| **Leptons** | Electron | $e^-$ | Charge: $-1$, Mass: $\sim 0.511$ MeV |
| | Electron Neutrino | $\nu_e$ | Charge: 0, Mass: $< 2.2$ eV |
| | Muon | $\mu^-$ | Charge: $-1$, Mass: $\sim 105.7$ MeV |
| | Muon Neutrino | $\nu_\mu$ | Charge: 0, Mass: $< 0.17$ MeV |
| | Tau | $\tau^-$ | Charge: $-1$, Mass: $\sim 1.777$ GeV |
| | Tau Neutrino | $\nu_\tau$ | Charge: 0, Mass: $< 15.5$ MeV |
| **Gauge Bosons** | Photon | $\gamma$ | Mediates electromagnetic force, Mass: 0 |
| | W Boson | $W^\pm$ | Mediates weak force, Mass: $\sim 80.4$ GeV |
| | Z Boson | $Z^0$ | Mediates weak force, Mass: $\sim 91.2$ GeV |
| | Gluon | $g$ | Mediates strong force, Mass: 0 |
| | Higgs Boson | $H$ | Gives particles mass, Mass: $\sim 125$ GeV |

Table 1: Summary of the Standard Model of Particle Physics

Particles are divided into two main categories: matter particles and gauge bosons. The former type, matter particles, can be divided further into two categories: quarks and leptons. Quarks form hadrons – familiar examples of which are protons and neutrons – and interact via the strong force; whereas leptons do not.

Matter particles are arranged in what are known as *generations*, which are groups of particles with similar properties. Each generation is composed of a pair of quarks and a pair of leptons. The first generation is the lightest and does not decay, i.e. the up and down quarks and the electron and electron neutrino; while the third is the heaviest, i.e. the

top and bottom quarks, and the tau lepton and tau neutrino. A difference to note within the respective generations is, however, that neutrinos are considered to be of a negligible mass.

Having established the make-up of the fundamental particles of our cosmos, the SM also describes the functionality behind forces. Particles in the category known as gauge bosons are the medium through which forces are exchanged: the electromagnetic force is exchanged between particles through photons, the strong force through the gluon, and the weak force through the W and Z bosons.

A facet of interest in the SM has been a particle known as the Higgs boson, as seen in Table 1. It is the last of the gauge bosons, and is posited to give mass to all particles in the Standard Model. This particle and its properties will be investigated in this essay, both within the scope of the SM and beyond it.

### 1.2 The Higgs Boson

The Higgs boson, and its associated *Higgs field*, were postulated in the mid-20th century as a solution to the electroweak theory necessitating massless W and Z bosons. Providing mass to both bosons would result in breaking the fundamental symmetry of the theory. In order to account for this, a phenomenon known as *spontaneous symmetry breaking* was postulated.

In this mechanism, the symmetry of natural laws remains unchanged, but that of the physical system is broken. A familiar example of this would be a pencil placed on its tip on a surface. The laws of physics do not determine a predefined direction for the direction to fall in, but due to the instability of the system, it does fall in a specific direction. [2]

This situation is but an analogy for the process of giving mass by the Higgs boson.

The Higgs boson has a field known as the Higgs field associated with it, which permeates the universe. The potential of the field is thought to have a *mexican hat* shape [2], as seen below in Figure 1. Here, the Higgs potential was said to be introduced in the early universe at the blue point, which is is a local maximum; yet highly unstable.As the universe expanded and cooled, the Higgs potential spontaneously *rolled* to the minimum of the field at the red point, giving rise to the mass of the W bosons, Z bosons, and all other particles. The mechanism by which this occurs is known as a *coupling* of the Higgs field, the mathematical details of which are outside the scope of this paper [3]. The Higgs mechanism thereby provides mass to the known particles in the Standard Model.

Presently, the Higgs particle is predicted to have positive charge-parity symmetry and

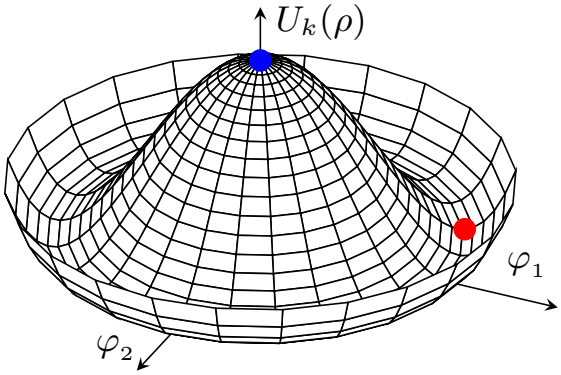


Figure 1: The Higgs Field's "Mexican Hat" Shape

zero spin [4]. The CP-symmetry of the Higgs ensures that interactions remain unchanged even when particles are replaced with their antiparticles and spatial coordinates are inverted.

## 1.3 Beyond the Standard Model

Despite the SM's success in various endeavours, it fails to explain the dominance of matter over antimatter in the universe, dark energy, dark matter, and most importantly, gravity. *Beyond the Standard Model Theories*, or BSM theories, may explain some of these unanswered questions, and typically predict new particles: such as more Higgs bosons. The existence of said particles implies differences in the currently discovered Higgs boson's behavior. By varying possibilities of quantum numbers and charge-parity violation of the Higgs boson, light can be shed on these new theories.

## 1.4 Theory

### 1.4.1 Standard Model Conditions

Covered in Section 1, the Higgs is known to have a spin of 0 and be CP-even in the Standard Model. Its subsequent coupling to the W bosons is shown by Equations 1 through 3 below. Equation 1 shows the Lagrangian – a way to express the HWW coupling – of the Standard Model; governing the dynamics of particles in the Higgs field.

In order to relate the following theory to data, we must go over the key points of the Higgs field and how couplings relate to experimental observations. The Higgs field is what is known as a complex $SU(2)_L$ doublet [6], given below:

$$\Phi = \begin{pmatrix} \phi_+ \\ \phi_0 \end{pmatrix} \tag{1}$$

Here, $\phi_+$ is a positively charged component of the Higgs field, and $\phi_0$ is a neutral component of the Higgs field, given by the following equation:

$$\phi_0 = \frac{1}{\sqrt{2}}(v + H + i\chi) \tag{2}$$

Where $v$ is the *vacuum expectation value*, explained later in this section; $H$ is the physical Higgs boson, which is a scalar particle; and $\chi$ is the Goldstone boson, which is later absorbed to give mass to the W bosons.

This field has a potential $V$ that is given by [6]:

$$V(\Phi) = \mu^2|\Phi|^2 + \lambda|\Phi|^4 \tag{3}$$

This is the function that gives rise to the aforementioned Mexican hat shape [6]. When relating the field to other particles, we describe their interactions using what is known as the *Lagrangian*, given by Equation 4.

$$\mathcal{L}_{SM} = |D_\mu \Phi|^2 \tag{4}$$

Here, $D_\mu$ is the covariant derivative, given [7, 6] by Equation 5:

$$D_\mu = \Big(\partial_\mu - i\frac{g}{2}\tau^a W_\mu^a - i\frac{g'Y}{2}B_\mu\Big) \tag{5}$$

$\partial_\mu$ here is the variation of spacetime; $\tau^a$ are the Pauli matrices, which describe the generators of $SU(2)_L$ symmetry; $W_\mu^a$ are the gauge W bosons associated with $SU(2)_L$; $g$ is a coupling constant for $SU(2)_L$; $B_\mu$ is the gauge boson associated with $U(1)_Y$; and $g'$ is the coupling constant for $U(1)_Y$. To calculate the Lagrangian for the Higgs-$W$ couplings, we can substitute this derivative into Equation 4.

$$\mathcal{L}_{SM} = |D_\mu \Phi| = \Big(\partial_\mu \Phi - i\frac{g}{2}\tau^a W_\mu^a \Phi - i\frac{g'}{2}B_\mu \Phi\Big)^\dagger \Big(\partial^\mu \Phi - i\frac{g}{2}\tau^a W^{\mu a}\Phi - i\frac{g'}{2}B^\mu \Phi\Big) \tag{6}$$

The process of substitution is not entirely straightforward, because $\Phi$ is a vector. To get a scalar product, the Hermitian conjugate – a row vector – of $D_\mu \Phi$ denoted by $\dagger$ is multiplied with the column vector $D^\mu \Phi$. The Lagrangian also must be found when the Higgs field breaks symmetry, as described in Section 1.2. The field gets what is known as a *vacuum*

*expectation value*, $v$, or a minimum potential as shown in Figure 1. In doing so and substituting the necessary parts of the equation, computation leads to Equation 8.

$$\langle \Phi \rangle = \begin{pmatrix} \phi_+ \\ \phi_0 \end{pmatrix} \rightarrow \frac{1}{\sqrt{2}} \begin{pmatrix} 0 \\ v \end{pmatrix}, v \approxeq 246 \text{ GeV} \tag{7}$$

$$\mathcal{L}_{SM} = \underbrace{\frac{g^2 v^2}{4} W_\mu^+ W_\mu^-}_{\text{mass term}} + \underbrace{\frac{g^2 v}{2} H W_\mu^+ W_\mu^-}_{\text{Higgs–W coupling}} + \underbrace{\frac{g^2}{4} H^2 W_\mu^+ W_\mu^-}_{\text{HHWW quartic vertex}} \underbrace{- \frac{1}{4} W^a \mu\nu W^{a\mu\nu} - \frac{1}{4} B_{\mu\nu} B^{\mu\nu}}_{\text{kinetic terms}} \tag{8}$$

Equation 8 gives the final Lagrangian for the Higgs-W boson couplings in the Standard Model [7, 8]. In the next section, we will explore the addition of further terms which affect charge-parity.

### 1.4.2 Beyond Standard Model Conditions

This paper explores a specific case of beyond-SM conditions; known as charge-parity violation, or CP-violation. Charge parity violation consists of two components; the first being charge symmetry.

**Charge symmetry**

is a property of a system that states that under the reversal of the charges on every involved particle, interactions remain unchanged.

**Parity symmetry**

is a property of a system that states that under the reversal of spatial coordinates on every involved particle, interactions remain unchanged.

In the Standard Model, the Higgs sector is entirely CP-even; meaning that charge and parity symmetry is respected [9]. However, we can introduce terms in the Lagrangian that break this symmetry, as seen in Equation 9 [10, 11, 12].

$$\begin{aligned} \mathcal{L}_{BSM} = & \underbrace{\frac{g^2 v}{2} H W_\mu^+ W^{\mu-}}_{\text{Standard Model Coupling}} + \underbrace{\frac{c_{HW} g^2}{\Lambda^2} H W_{\mu\nu}^+ W^{\mu\nu-}}_{\text{CP-Even Modification}} \\ & + \underbrace{\frac{\tilde{c}_{HW} g^2}{\Lambda^2} H W_{\mu\nu}^+ \tilde{W}^{\mu\nu-}}_{\text{CP-Odd Modification}} \underbrace{- \frac{1}{4} W^a \mu\nu W^{a\mu\nu} - \frac{1}{4} B_{\mu\nu} B^{\mu\nu}}_{\text{kinetic terms}} \end{aligned} \tag{9}$$

Here, three new terms are added. $c_{HW}$ and $\tilde{c}_{HW}$ are known as *Wilson coefficients*, which act as magnitudes of the modifications to the charge-parity symmetry. These are the parameters that will be controlled in order to distinguish between distributions in the next section.

Next, $\Lambda$ is the energy scale of new physics: this is the value of energies beyond which these modifications stop being signficiant. It acts as a threshold for the modifications: the higher the value of $\Lambda$, the smaller the contribution of the new physics terms at low energies, making them harder to detect.

Finally, $W_{\mu\nu}$ is the field strength tensor, and $\tilde{W}_{\mu\nu}$ is the dual field strength tensor. Without delving into unnecessary detail, the field strength tensor describing the transformation of the gauge field $W_\mu$ under spacetime transformations. The dual field strength tensor achieves the same purpose, but incorporates asymmetry when transformed; as it switches signs.

Section 3.2 will explore how different magnitudes of the CP-even and CP-odd modifications affect certain key observables of the aforementioned diffractive production channel, whose Feynman diagram is seen in Figure 2.

### 1.5 Aim

In order to do so, this research focuses on the interaction between the Higgs boson and the W+ and W- bosons; or the HWW couplings. In doing so, we will explore one main diffractive production channel in SM and non-SM conditions; which is seen in Figure 2. In simple words, the diagram above shows the result from a collision of two protons. As they interact with the electromagnetic force, they exchange two photons. The two photons collide and form a pair of W bosons, both of which decay into pairs of leptons; and a Higgs boson, which decays into a pair of bottom quarks.

BSM CP-odd Higgs boson couplings to the W-bosons affect angular distributions in processes like $pp \to \gamma\gamma \to WWh$ [14]. By simulating and studying these distributions, we can search for observables that allow to distinguish between CP-even and CP-odd contributions, that can later be used experimentally in determining whether CP violation occurs in Higgs interactions.

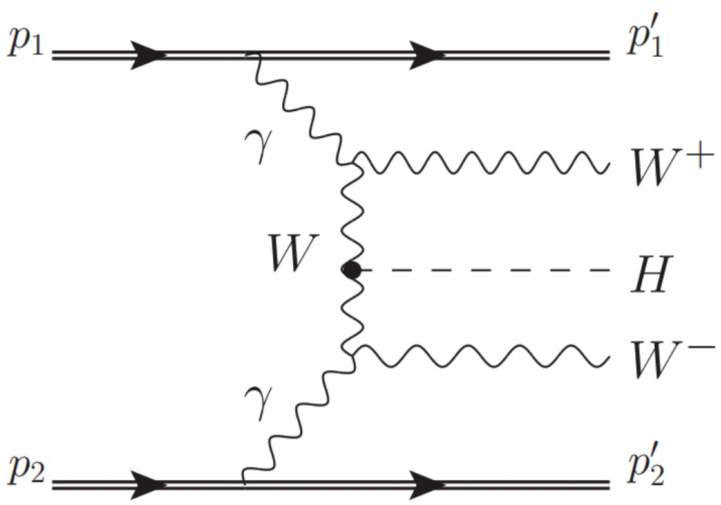


Figure 2: Feynman diagram of the $pp \to ppWWH$ diffractive production process [13]

# 2 Methodology

## 2.1 Tools

### 2.1.1 MadGraph

MadGraph is a software that allows for "the automated computation of tree-level and next-to-leading order differential cross sections, and their matching to parton shower simulations" [15]. I used it to generate the simulation data which was subsequently analysed in ROOT.

### 2.1.2 Universal FeynRules Output

that incorporates new theoretical parameters and interactions, allowing for the simulation of physics scenarios that deviate from SM predictions. In this study, the UFO model used is the *SMEFTsim_U35_MwScheme* framework, which introduces effective field theory operators that modify the Higgs-W boson coupling to test CP-even and CP-odd interactions [16].

### 2.1.3 ROOT

CERN's ROOT is a sophisticated piece of high-energy physics analysis software that aids the storage, processing, visualisation and analysis of scientific data [17]. I used ROOT in

order to plot kinematic observables of the MadGraph-produced data such as transverse momentum, pseudorapidity, and angular distribution.

### 2.2 Procedure

To achieve the aim set forth in this paper, I analysed the transverse momentum, pseudorapidity, and basic angular distributions of particles in the chosen diffractive production channel – once under Standard Model conditions, and in four different non-Standard Model scenarios with varying charge-parity assumptions. These assumptions will be controlled by Wilson coefficients, namely $c_{HW}$ and $\tilde{c}_{HW}$. $c_{HW}$ increases the probability of even-CP behaviour, which is set to either $+0.5$ and $-0.5$, whereas $\tilde{c}_{HW}$ increases the probability of CP-odd behaviour, and is set to either $-1.2$ or $1.2$. An important aspect is that we consider the energy scale of this new physics, $\Lambda$, to be 1 TeV. These distributions will be studied as a function of the kind of HWW couplings in order to find key markers and characteristics which can be observed in future experimental data.

## 3 Results and Discussion

### 3.1 Comparisons and Analysis

#### 3.1.1 Transverse Momentum

Transverse momentum is a measure of a particle's momentum perpendicular to the beamline. In theory: Increasing coupling strength – by keeping $c_{HW}$ values positive – would create a narrower, taller, and right-shifted peak in the distribution, whereas decreasing the coupling strength – by keeping $c_{HW}$ values negative – would flatten the distribution, dull the peak, and shift it leftwards. Alterations to $\tilde{c}_{HW}$[1] change the probability of producing $H$ and $W$ bosons with high transverse momentum.

**Observations**

The transverse momenta of all three bosons follow certain key features in all five conditions. Firstly, a large amount of entries exist at a low transverse momentum, close to 75 GeV. The density of events at higher transverse momenta begins to decrease compared to the peak. Where these qualities mainly differ between conditions is peak height. SM conditions and negative $\tilde{c}_{HW}$ conditions follow a nearly identical pattern; whereas both positive and negative $c_{HW}$ conditions see a flatter distribution of events; and positive $\tilde{c}_{HW}$ conditions spurs data that is uniformly distributed. This property is characteristic of CP-odd events, which means that a larger number of events at high transverse momentum in real data could signal towards CP-violation.

[1]Note that on distributions, $\tilde{c}_{HW}$ is referred to as *cHWtil*.

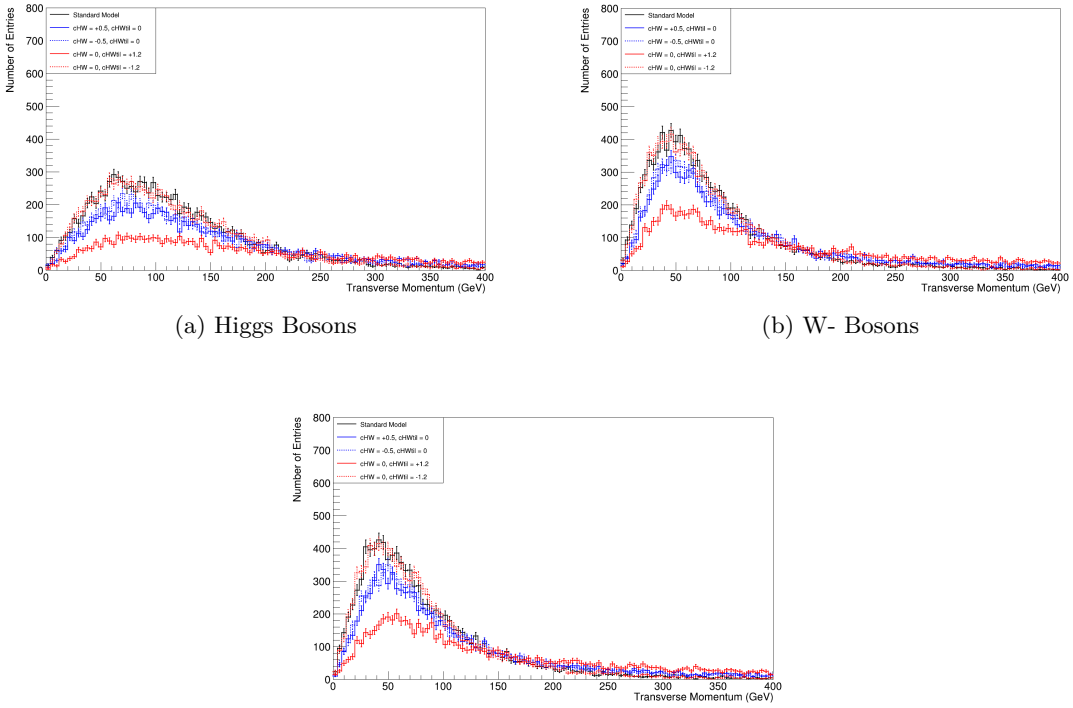


(a) Higgs Bosons

(b) W- Bosons

(c) W+ Bosons

Figure 3: Distribution of the transverse momentum of the particles involved in the SM WWH diffractive production in black and for two BSM scenarios with increased CP-even coupling in blue and CP-odd coupling in red

### 3.1.2 $\Delta\eta$

$\Delta\eta$ is a calculated property, equal to the difference in pseudorapidity between a pair of a lepton and its antilepton. This is somewhat analogous to the angle subtended between the path of each particle, parallel to the beam axis. Theoretically, deviations from the SM in terms of charge-parity violation can drastically change the distribution of $\Delta\eta$ as interactions between particles and anti-particles will no longer undergo similar interactions. The explorations can be seen below.

#### Observations

Figure (a) shows the effects of changing $c_{HW}$ on the $\Delta\eta$ distributions. In the Standard Model, two peaks are seen at the values of around -5 and 5, and a local minimum at 0.

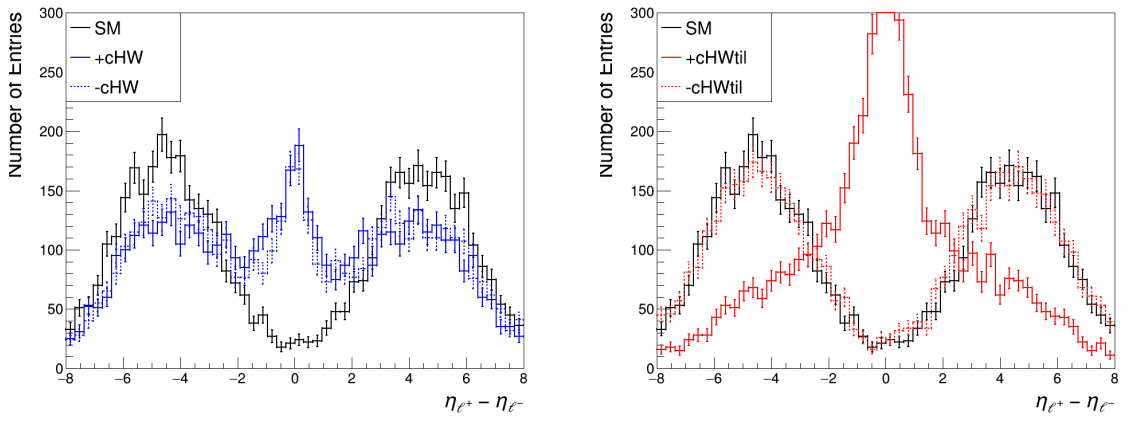


(a) $\pm c_{HW}$ (b) $\pm \tilde{c}_{HW}$

Figure 4: Distribution of the pseudorapidity difference between the charged leptons coming from the W-boson decays for the SM WWH diffractive production in black and for two BSM scenarios with increased CP-even coupling in blue and decreased CP-odd coupling in red.

This means that very few lepton-antilepton pairs are ejected from the collision in the same direction. However, both reducing and increasing the CP-even term $c_{HW}$ dramatically increases the number of events at 0 $\Delta\eta$, and decreases the peaks at -5 and 5. Hence, a larger number of lepton-antilepton pairs travelled in the same direction, and less were highly separated. More unidirectional jets could be observed in both cases. However, increasing CP-odd terms creates significantly different event topology: as can be seen in Figure (b), an immensely large peak is seen at $\Delta\eta = 0$, compared to the minimum in Standard Model conditions. Decreasing the CP-odd term makes minimal differences in the distribution. Hence, a strong sign of CP-violation in physics data would be very dense particle jets in the same direction.

### 3.1.3 $\Delta\phi$

$\Delta\phi$ is similar to $\Delta\eta$, but instead measures the azimuthal angular distribution between a lepton and an antilepton perpendicular to the beam axis.

#### Observations

In both plots, we can see very minimal changes in distributions. In Figure (a), it can be seen that in Standard Model conditions, a relatively flat distribution is seen with a slight peak near $\Delta\phi = 0$, showing a marginally higher number of lepton-antilepton pairs being

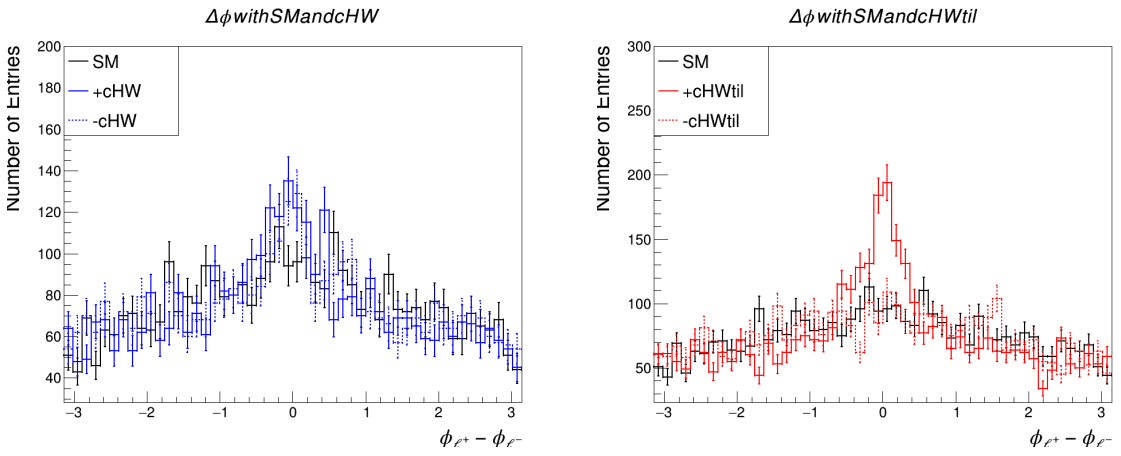


(a) $c_{HW}$ (b) $c_{\tilde{HW}}$

Figure 5: Distribution of the azimuthal angle difference between the charged leptons coming from the W-boson decays for the SM WWH diffractive production in black and for two BSM scenarios with increased CP-even coupling in blue and CP-odd coupling in red.

ejected along the same angle perpendicular to the beam axis. However, increasing the CP-even terms $c_{HW}$ narrows the distribution and creates a higher peak at $\Delta\phi = 0$, showing a higher number of lepton-antilepton pairs being ejected at the same angle. Decreasing the CP-even terms has the same impact. This can be seen also in the CP-odd terms; the same effect is seen in both decreasing and increasing the terms. Increasing CP-violating effects creates an exacerbated peak at $\Delta\phi = 0$, more significantly than CP-even terms. Decreasing CP-odd terms harbors nearly no effects, creating a distribution similar to that of the Standard Model.

### 3.1.4 Pseudo-Rapidity

As discussed above, pseudo-rapidity is a measure of the angular separation of a particle parallel to the beam axis. The distributions below can give insight into not the relative separation of particles and anti-particles, but the overall topology of the event.

#### Observations

The Higgs bosons are mostly ejected centrally in the detector, with $|\eta| \lessapprox 2$. There are no notable differences between the five configurations of CP-even and CP-odd terms, but there is a higher proportion of centrally produced Higgs bosons at$\eta = 0$ in the CP-odd terms.

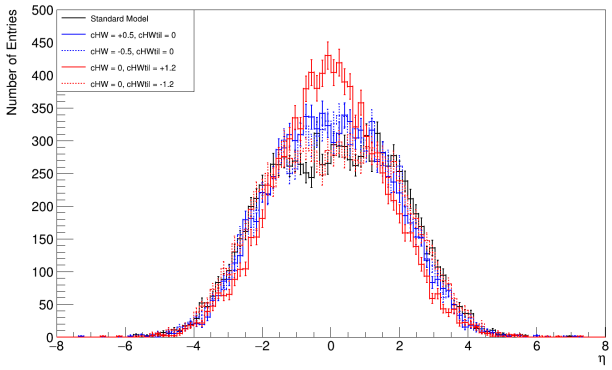


(a) Higgs Bosons

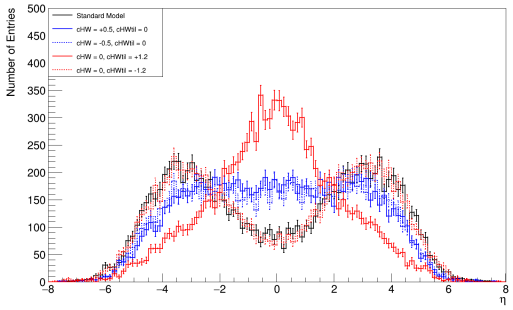


(b) W- Bosons

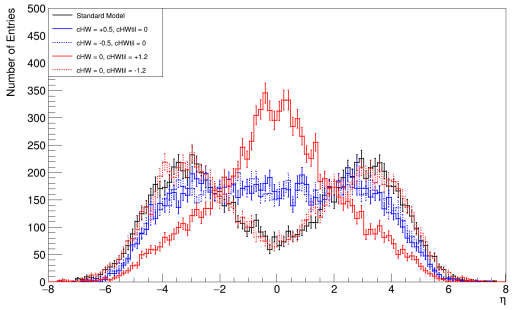


(c) W+ Bosons

Figure 6: Distribution of the transverse momentum of the particles involved in the SM WWH diffractive production in black and for two BSM scenarios with increased CP-even coupling in blue and CP-odd coupling in red

As for the W- bosons, the Standard Model and lowered CP-odd terms exhibit similar plots. Both show a minimum at $\eta = 0$, and two maxima around $\eta = -4$ and $\eta = 4$. This indicates that there are multiple W- bosons ejected along the beam axis, whereas few were ejected perpendicular to the beam axis. Both CP-even configurations show flatter plots, showing an even distribution of W- bosons in both cases parallel to the beam. However, an increased CP-odd term, shown by the solid red plot, shows a drastic difference: a high peak at $\eta = 0$, indicating a very large proportion of W-bosons being ejected nearly perpendicular to the beam. This is a sign to search for in physical data of CP-violation taking place.The W+ bosons exhibit the same distributions as the W- bosons.

# 4 Conclusion

In the search for charge-parity violation with respect to Higgs boson decay processes, the results indicate several key pointers to look out for in data. For one, flatter and varied distributions in the transverse momentum of all involved particles point towards CP-violation. Furthermore, smaller separation between lepton-antilepton pairs is a cornerstone in this configuration both along the beam axis as well as perpendicular to the beam axis. Theoretically, a large number of ejected W+ and W- bosons perpendicular to the beam axis is a crucial component of CP-violation. The full shape of the $\Delta\eta_{e^+e^-}$ plot can also be used to distinguish between CP-even and CP-odd couplings in the HWW interactions..

# 5 Acknowledgements

I would like to acknowledge that in order to facilitate my work, I was granted access to a variety of software tools by LIP Portugal. Special thanks to Prof. Patricia Conde, researcher at LIP Portugal and the CERN ATLAS experiment, for guiding my work.

# References

[1] Mary K. Gaillard, Paul D. Grannis, and Frank J. Sciulli. The standard model of particle physics. *Rev. Mod. Phys.*, 71:S96–S111, Mar 1999.

[2] Suzanne van Dam. Spontaneous symmetry breaking in the higgs mechanism. This essay was submitted as part of the Master's course "Part III of the Mathematical Tripos" at the University of Cambridge.

[3] Ahmed Abokhalil. The higgs mechanism and higgs boson: Unveiling the symmetry of the universe, 2023.

[4] Heather Gray and Bruno Mansoulié. The higgs boson: The hunt, the discovery, the study and some future perspectives. `https://atlas.cern/updates/feature/higgs-boson`, 2018. Accessed: 2024-11-28.

[5] Wikipedia Contributors. Two-higgs-doublet model (2hdm). *Wikipedia*, 2023.

[6] John F. Gunion, Howard E. Haber, Gordon L. Kane, and Sally Dawson. *The Higgs Hunter's Guide*. Perseus Publishing, 2000.

[7] Steven Weinberg. Baryon- and lepton-nonconserving processes. *Physical Review Letters*, 43:1566–1570, 1979.

[8] Michael E. Peskin and Daniel V. Schroeder. *An Introduction to Quantum Field Theory*. Westview Press, 1995.

[9] Aqeel Ahmed. Phenomenology of cp-violating higgs and gauge-boson couplings. *PMC Journal*, 10:35–42, 2021.

[10] Aqeel Ahmed and Asim Khan. Cp-violating higgs and gauge boson couplings in the smeft framework. *PMC Journal*, 11:22–30, 2022.

[11] B. Grzadkowski, M. Iskrzynski, M. Misiak, and J. Rosiek. Dimension-six terms in the effective lagrangian. *Journal of High Energy Physics*, 2010:085, 2010.

[12] J. A. Aguilar-Saavedra and M. Perez-Victoria. Effective lagrangians for higgs-gauge interactions. *Physical Review D*, 100:095012, 2019.

[13] CMS Collaboration. The cms precision proton spectrometer at the hl-lhc – expression of interest, 2021.

[14] Particle Data Group. The higgs boson. *Progress of Theoretical and Experimental Physics*, 2021:083C01, 2021.

[15] J. Alwall, R. Frederix, S. Frixione, V. Hirschi, F. Maltoni, O. Mattelaer, H.-S. Shao, T. Stelzer, P. Torrielli, and M. Zaro. The automated computation of tree-level and next-to-leading order differential cross sections, and their matching to parton shower simulations. *Journal of High Energy Physics*, 2014(7), July 2014.

[16] Ilaria Brivio. Smeftsim 3.0 — a practical guide. *Journal of High Energy Physics*, 2021(4), April 2021.

[17] René Brun and Fons Rademakers. ROOT - An Object Oriented Data Analysis Framework. *Nuclear Instruments and Methods in Physics Research Section A*, 389:81–86, 1997. Proceedings of AIHENP'96 Workshop, Lausanne, Sep. 1996. Software: ROOT, Release v6.24/06, launched 3 Sep 2021.